Chiral Optical Scattering from Helical and Twisted Silica Nanoribbons

Peizhao Liu,[a,b] Yann Battie,[c] Yutaka Okazaki,[b] Naoya Ryu,[d] Emilie Pouget,[a] Sylvain Nlate,[a]

Takashi Sagawa,*[b] and Reiko Oda*[a]

[a] CNRS, University of Bordeaux, Bordeaux INP, Chimie et Biologie des Membrance et des Nanoobjets (CBMN), UMR 5248, 33607, Pessac, France

[b] Graduate School of Energy Science, Kyoto University, 606-8501, Kyoto, Japan

[c] Université de Lorraine, Laboratoire de Chimie et Physique - Approche Multi-échelles des milieux Complexes, (LCP-A2MC), 1 Boulevard Arago, 57078 Metz, France.

[d] Materials Development Department, Kumamoto Industrial Research Institute, 3-11-38 Higashimachi, Higashi-ku, Kumamoto 862-0901, Japan.

Experimental details

Materials and instrumentations

All chemicals were of reagent grade and purchased from chemical suppliers. *N,N'*-Dihexadecyl-*N,N,N',N'*-tetramethylethylene diammonium L- (and D-) tartrate (16-2-16 L- (and D-) tartrate) were synthesized by the previously reported procedure [1, 2].

Preparation of colloidal suspension of silica nanoribbons

5 mL of 16-2-16 L- (and D-) tartrate (1 mM) aqueous solution was heated at 60 ˚C to be clear solution. After cooled it down at 20 ˚C for 3 days, 5 mL of prehydrolyzed TEOS aqueous solution (TEOS : water = 1 : 20 v/v) containing 0.1 mM L- (and D-) tartaric acid was added to the 16-2-16 L- (and D-)

tartrate aqueous solution and the mixture was kept at 20˚C for 18 hs. Unreacted TEOS was removed by washing with methanol at 60 ˚C using centrifuge (3000-4000*g*, 5 min.). Completion of each washing process was confirmed by weight of dried supernatant, UV-visible and ^{1}H-NMR spectra. After exchanging the solvent of the obtained suspension from methanol to ethanol by centrifugation (3000-4000*g*, 5 min.), ultrasonic processor (Vibra-Cell 75186) equipped with 6 mm microtip with variable power was used to obtained homogeneous colloidal suspension (maximum power, 130 W). A 20 kHz pulse mode was used for the dispersion and fragmentation of silica helical and twisted nanoribbons. Concentration of the colloidal suspension of silica nanoribbons was adjusted to be 1.0 mg mL^{-1} and kept at 4 ˚C for the experiments.

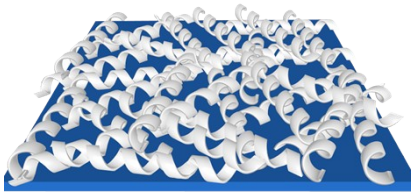

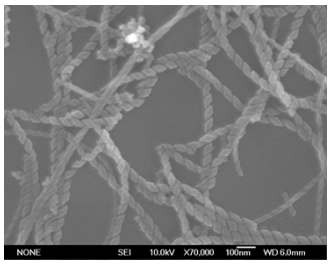

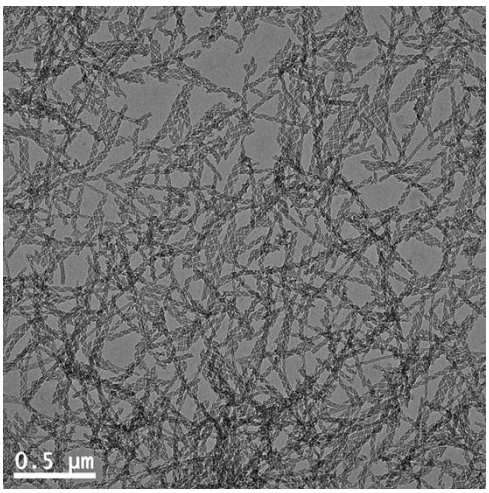

Preparation of silica nanoribbon films

The quartz substrates (2 cm × 2 cm) were washed with milli-Q water, acetone, and isopropanol in turn with sonication for 30 min. The washed quartz substrates were kept in isopropanol for further use. 100 µL, 200 µL, 400 µL, 600 µL, and 800 µL of colloidal silica nanohelices (1.0 mg mL^{-1}) ethanol suspension were drop-casted on the quartz substrate. After drying under air at room temperature, the obtained silica nanohelices films were used for various spectral measurements. For calcination of silica nanoribbons films, the temperature was increased from 25 ℃ to 900 ℃ with 9

hours and kept at 900 ℃ for 2 h.

Transmission electron microscopy (TEM) observation

A drop (ca. 5 μL) of the sample solution was casted on the grid. The excess solution was removed with filter paper, and the grid was air-dried. After vacuum drying, these grids were used for TEM observation. TEM observation was performed with a Philips EM 120 electron microscope operating at 120 kV, and the images were collected with a 2k × 2k Gatan ssCCD camera.

Field emission scanning electron microscopy (FE-SEM) observation

The silica nanoribbon films were put on the stage in the horizontal and vertical directions using conductive carbon adhesive tape for surface observations and cross-section observations, respectively. After coated by gold for 30 seconds using magnetron sputter MSP-mini (Vacuum Device), these specimens were used for FE-SEM observations. FE-SEM observations were performed with a SU6600 (Hitachi High-Technologies) at 15 kV.

The SEM of Figure S1 was performed on a JSM 6700F JEOL operating at 10kV after covering the sample with aAu/Pt layer with a thickness of a few nanometers.

CD spectral measurements in the transmission mode (TCD)

CD, LD, and UV-visible absorption spectral measurements in the transmission mode were carried out by using J-1500 (JASCO). All the samples were measured with two angles (0 °and 90°) rotated around the light beam axis. The final CD spectra were obtained by the mean values of data measured at 0° and 90°. The LD is also measured with two angles (0 °and 90°) to know whether LD affects the CD or not.

CD spectral measurements in the diffuse reflection mode (DRCD)

CD, LD, and UV-visible absorption spectral measurements in the transmission mode were carried out by using J-1500 (JASCO) with integration sphere attachment (DRCD-575). The DRCD spectra in Figures 1g and 1h were corrected by the following set up A with white background. The DRCD spectra in Figures S11 and S12 were corrected by the following set up B and C, respectively.

Table S1 Dimensions of the silica nanoribbons. Some values were taken from our previous publications.[18,35] To obtain the dimensions of the twist ribbons after calcination which is difficult to clearly determine due to their small sizes, same shrinking ratios are taken as helical ribbons for the width, thickness pitch and length respectively and applied to the sizes before the calcination.

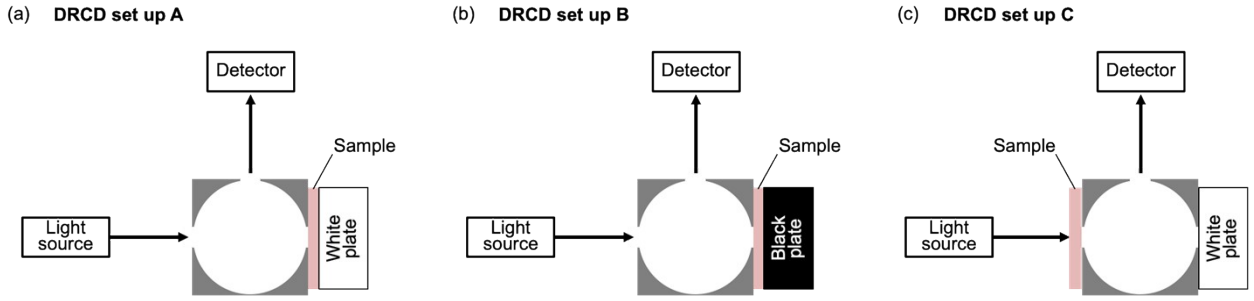

Theoretical analysis

The extinction and scattering cross section of individual silica helices and twist ribbons are simulated according to the boundary element method (BEM).[3] This method requires to discretize the surface of the nanostructure. More than 5000 vertices are used to define each nanostructure surface. The dielectric function of silica is given by E. D. Palik [4] while air is used as the ambient medium. The incident light is parallel or perpendicular to the helices/twist ribbons orientation. The extinction (σ_{ext}) and scattering (σ_{scat}) cross sections are simulated for LH- and RH- circular polarizations. The extinction and scattering cross sections of nanostructures for non-polarized light are calculated from the following equation:

$$\sigma_{ext/scat} = \frac{\sigma_{ext/scat,L} + \sigma_{ext/scat,R}}{2} \quad (1)$$

with $\sigma_{ext/scat,L}$ and $\sigma_{ext/scat,R}$ are the extinction or scattering cross obtained for LH- and RH- circular polarization, respectively. The circular dichroism (CD_{ext}) is deduced from the following equation:

$CD_{ext} = \sigma_{ext,L} - \sigma_{ext,R}$. (2)

CD_{ext} is the sum of two contributions:

$CD_{ext} = CD_{scat} + CD_{abs}$. (3)

The first term of equation 3 is the dichroism induced by the chiral scattering (CD_{scat}) while the second term is related to the difference in the absorption of LH- and RH- CP light (CD_{abs}). The g-factor is estimated from the ratio between the CD_{ext} and the extinction cross section σ_{ext}.

	Width	Thickness	Pitch	Length	Diameter
Twist before calc.	19.4 ± 3.8 nm	12.2 ± 2.3 nm	88.6 ± 14.0 nm	500 nm	19.4 ± 3.8 nm (= Width)
Twist after calc. at 900 ˚C	16.7 ± 3.3 nm*	12.0 ± 2.2 nm*	69.2 ± 10.9 nm*	390 nm	16.7 ± 3.3 nm (= Width)
Ratio after/before	86.3%	98.2%	78.1%	78.1% (= Pitch)	86.3% (= Width)
Helical before calc.	26.2 ± 2.4 nm	11.4 ± 1.4 nm	58.0 ± 12.4 nm	500 nm	27.1 ± 4.2 nm
Helical after calc. at 900 ˚C	22.6 ± 2.2 nm	11.2 ± 1.0 nm	45.3 ± 8.8 nm	390 nm	24.4 ± 3.4 nm
Ratio after/before	86.3%	98.2%	78.1%	78.1% (= Pitch)	90.0%

Supplementary figures

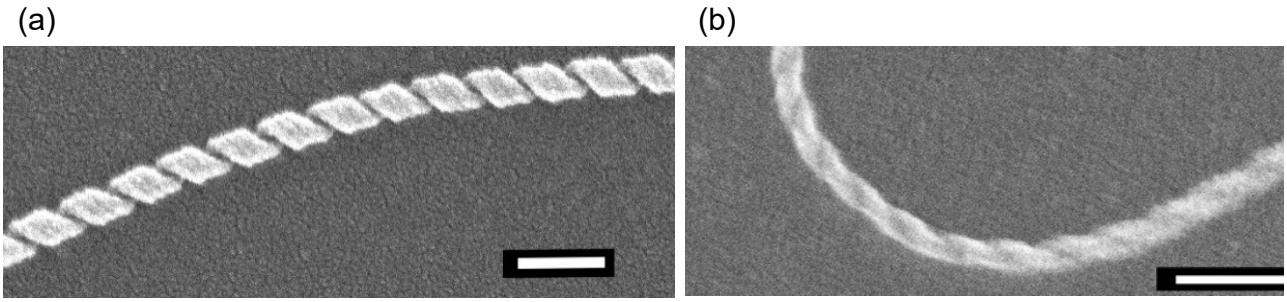

Figure S1 SEM images of RH- (a) helical and (b) twisted silica nanoribbons. Scale bars are 100 nm.

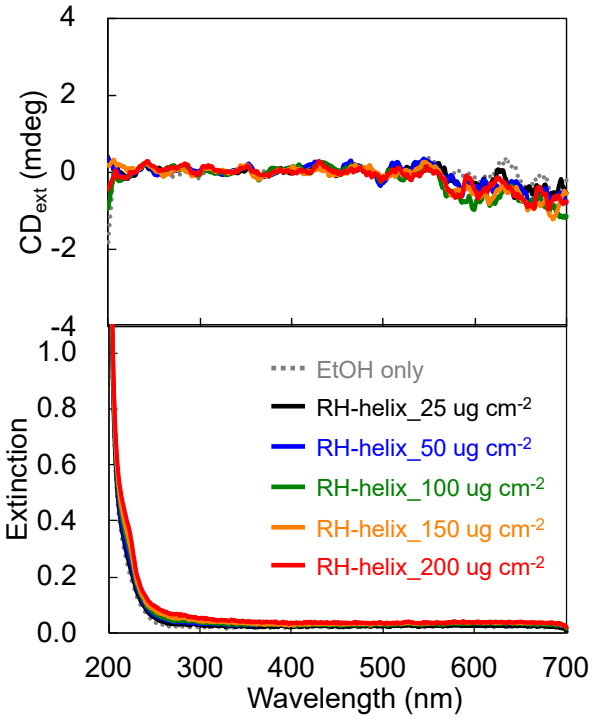

Figure S2 CD_{ext} (top) and extinction (botom) spectra of helical silica nanoribbon in ethanol. All spectra were measured by using 1 cm quartz cell (bottom area: 1 cm × 1 cm). To compare with film samples, 50 μg (25 μg cm^{-2}), 100 μg (50 μg cm^{-2}), 200 μg (100 μg cm^{-2}), 300 μg (150 μg cm^{-2}), and 400 μg (200 ug cm^{-2}) of RH-helical silica nanoribbons were suspended in 2 mL of EtOH, respectively.

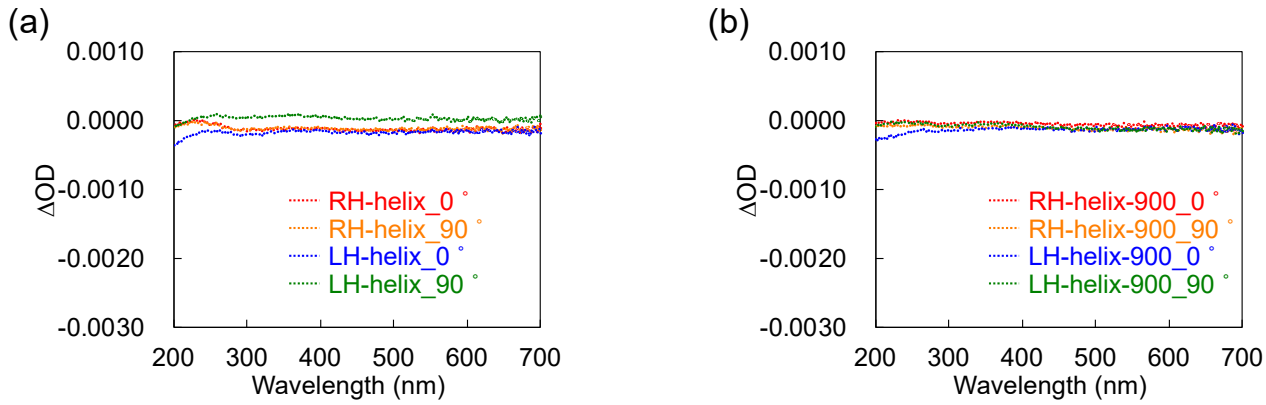

Figure S3 LD spectra of helical silica nanoribbon films (a) before and (b) after calcination at 900 ˚C. All spectra were recorded by CD spectrometer on the transmission mode. All films were measured at two angles (0 ˚ and 90 ˚) rotated around the light beam axis.

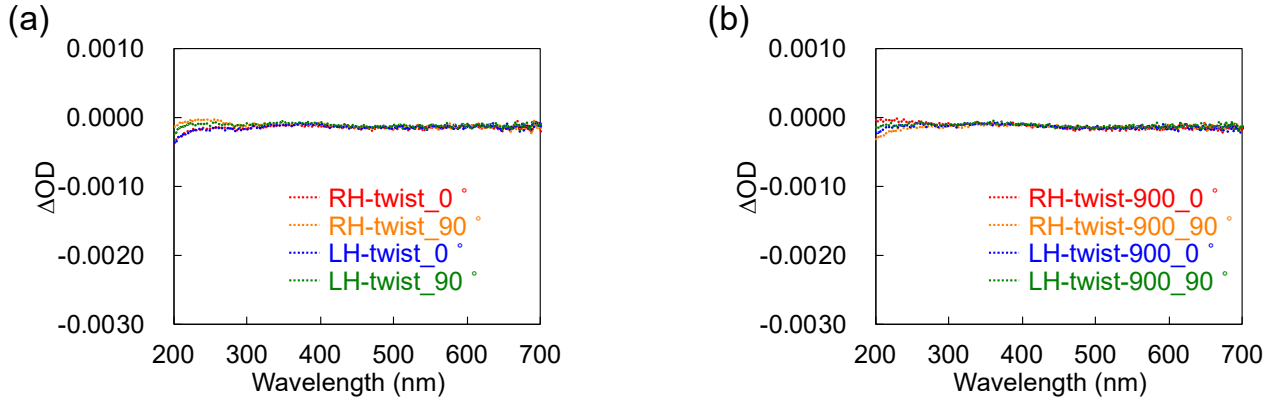

Figure S4 LD spectra of twisted silica nanoribbon films (a) before and (b) after calcination at 900 ˚C. All spectra were recorded by CD spectrometer on the transmission mode. All films were measured at two angles (0 ˚ and 90 ˚) rotated around the light beam axis.

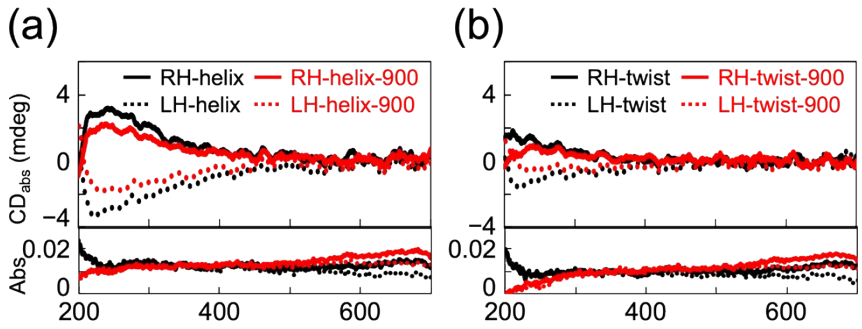

Figure S5 CD_{abs} (top) and absorption (bottom) spectra of drop-casted films (50 µg cm^{-2}) of (a) helical and (b) twisted silica nanoribbons. All spectra were measured by DRCD measurement setup A.

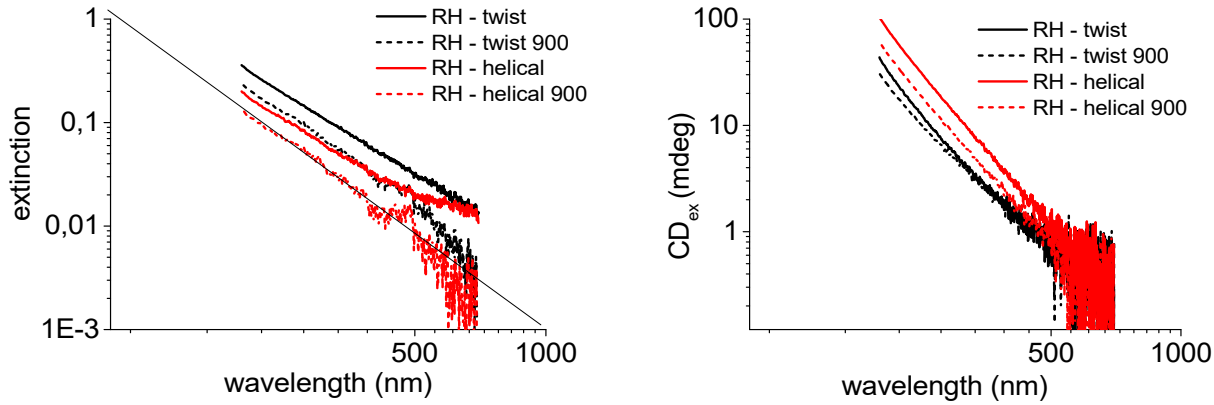

Figure S6 Log-log plots of scattering cross section and CD_{scat} of RH-helical and twist ribbons before and after calcination at 900°C

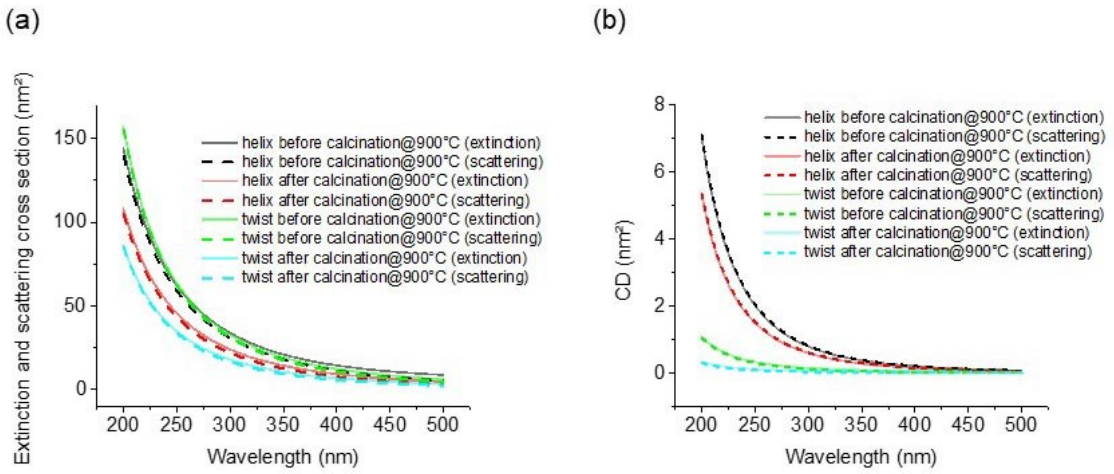

Figure S7 Simulation data of extinction and CD_{ext} as well as scattering cross section and CD_{scat} values of helical and twisted ribbons before and after calcination at 900°C.

In order to see how twist and helical ribbons can scatter light, we investigated how the vectors representing the normal to the silica surface change directions along the ribbons.

The structures are modeled as opened surfaces. The position of a point M on a twist ribbon, with width *2r* and pitch *p*, is described by the following parametric equations:

$M(t,\mu) = \begin{pmatrix} t\cos(\mu) \\ t\sin(\mu) \\ h\,\mu \end{pmatrix}$ with $t \in [-r,r]$ the radial coordinate and $2\pi h = p$.

a) b) c)

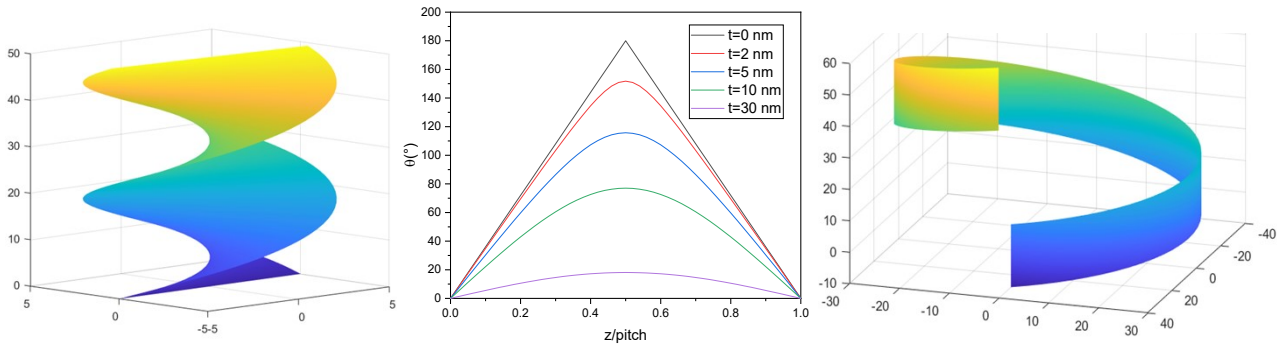

The figure S8 a) structure of twist ribbon obtained for p = 50 nm and r = 5. b) evolution of the angle θ with the height z and the radial coordinate t. c) Evolution of the angle θ with the height z and the radial coordinate t.

We quantify the local chirality of the structure by evaluating the angle $\theta(t,\mu)$ between the vectors perpendicular to surface at a point M(t,μ) and a point M(t,0) along the ribbon. This angle is given by:

$$\theta(t,\mu) = \text{acos}\left(\frac{h^2\cos(\mu) + t^2}{h^2 + t^2}\right) = acos(\frac{h^2\cos(z/h) + t^2}{h^2 + t^2})$$

The figures above show the evolution of this angle with the height z and the radial coordinate t.

The angle is maximized at the center of the twist ribbon (Figure S7(a) and (b)). In other words, the vector normal to the surface rotate more at the center of the ribbon than at the edge. Thus, edge is less chiral than the center. At the center, the angle is given by:

$\theta(0,\mu) = \mu$

In contrast, helical ribbon (Figure S7(c)) is created by a segment $2a$ which rotates with a radius r and pitch p. This structure is described by the following equations where the points M(t,μ) on the surface has coordinates :

$$M(t,\mu) = \begin{pmatrix} r\,cos(\mu) \\ r\,sin(\mu) \\ t + h\mu \end{pmatrix} with\ \ t \in [-a,a]\ while\ 2a\ is\ the\ width\ of\ and,\ 2\pi h = p$$

the vectors perpendicular to surface at a point M(t,μ) is given as : $\vec{n}(t,\mu) = \begin{pmatrix} r\,cos(\mu) \\ r\,sin(\mu) \\ 0 \end{pmatrix}$. This vector is independent of t.

We can again evaluate the angle $\theta(t,\mu)$ between the vectors perpendicular to surface at a point M(t,μ) and a point M(t,0) for this structure. This angle is given by

$\theta(t,\mu) = \mu$

this is valid for all t values (everywhere on the surface) of the helical ribbon. Whereas this value μ corresponds to the maximal value of twist ribbon only at the center of the ribbons as previously indicated. In other words, the surface of the twist ribbons are less chiral than that of helical ribbons.

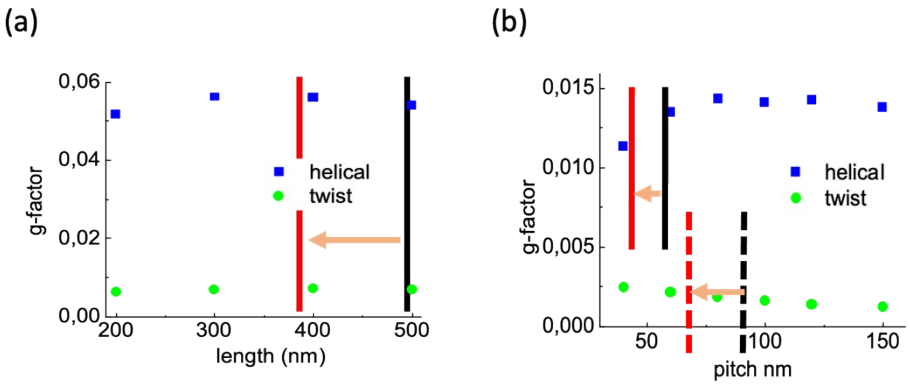

Figure S9 Variation of g-factors of helical and twisted nanoribbons as a function of (b) ribbons' length at a fixed diameter and pitches, and (c) pitches at a fixed length and diameter.

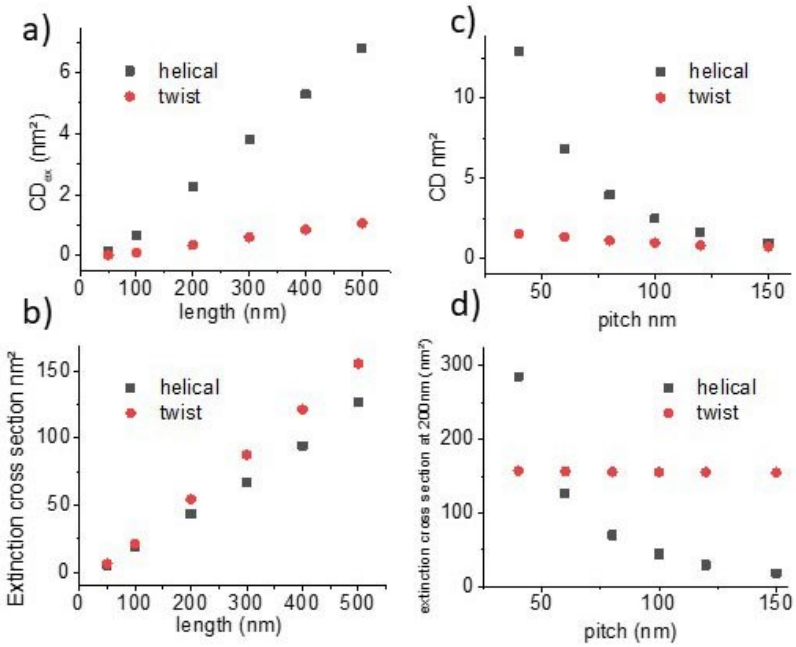

Figure S10 Simulated extinction and CD_{ext} at a wavelength of 200nm as a function of the length (at a fixed pitch and diameter) and the pitch (at a fixed length and diameter) respectively of a single helical or twisted ribbon

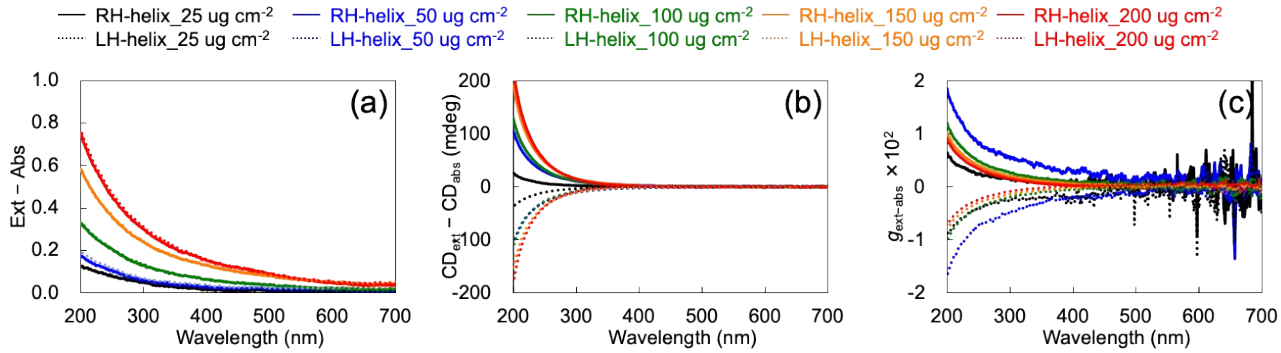

Figure S11 (a) Total scattering (Ext − Abs), (b) chiral scattering ($CD_{ext} - CD_{abs}$), and (c) g-factor of chiral scattering ($g_{ext-abs}$) spectra of silica nanohelices films with various quantities.

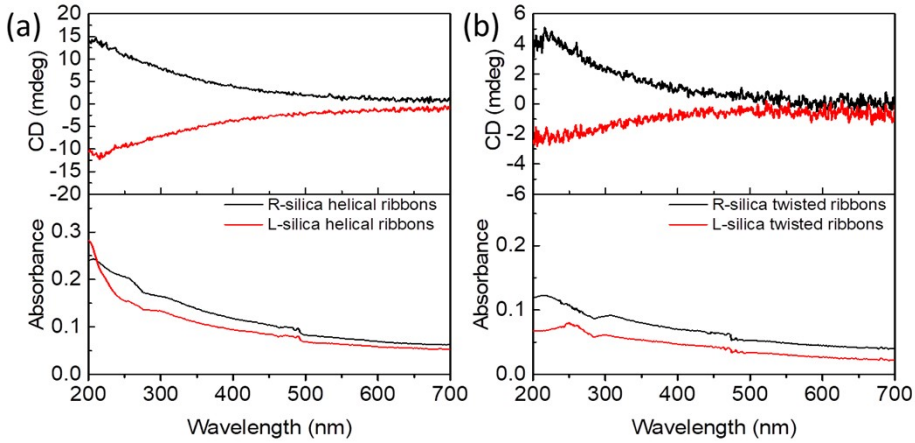

Figure S12 CD_{ext} (top), and extinction (bottom) spectra of non-cut (a) helical and (b) twisted silica nanoribbon films before the calcination (RH black lines and LH red lines). All spectra were recorded by CD spectrometer on the transmission mode. All films were measured at two angles (0 ˚ and 90 ˚) rotated around the light beam axis.

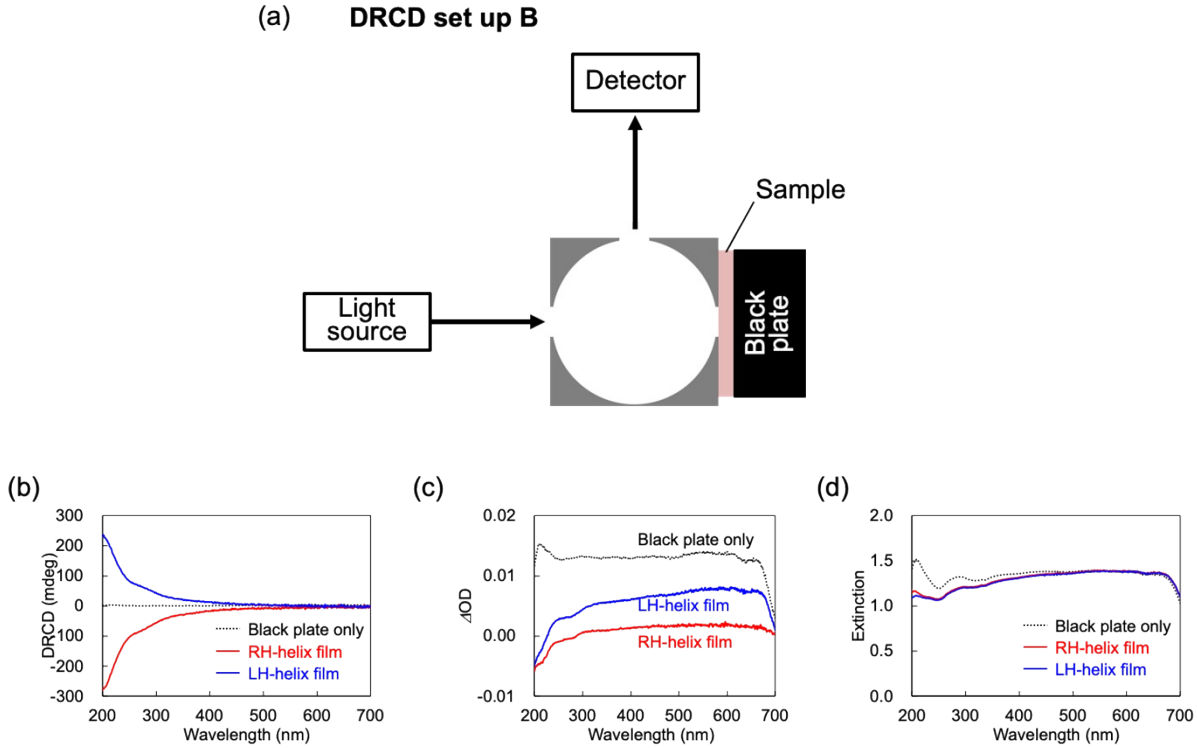

Figure S13 (a) Schematic illustration of DRCD measurement set up B. (b) CD, (c) LD, and (d) extinction spectra of silica nanohelices films.

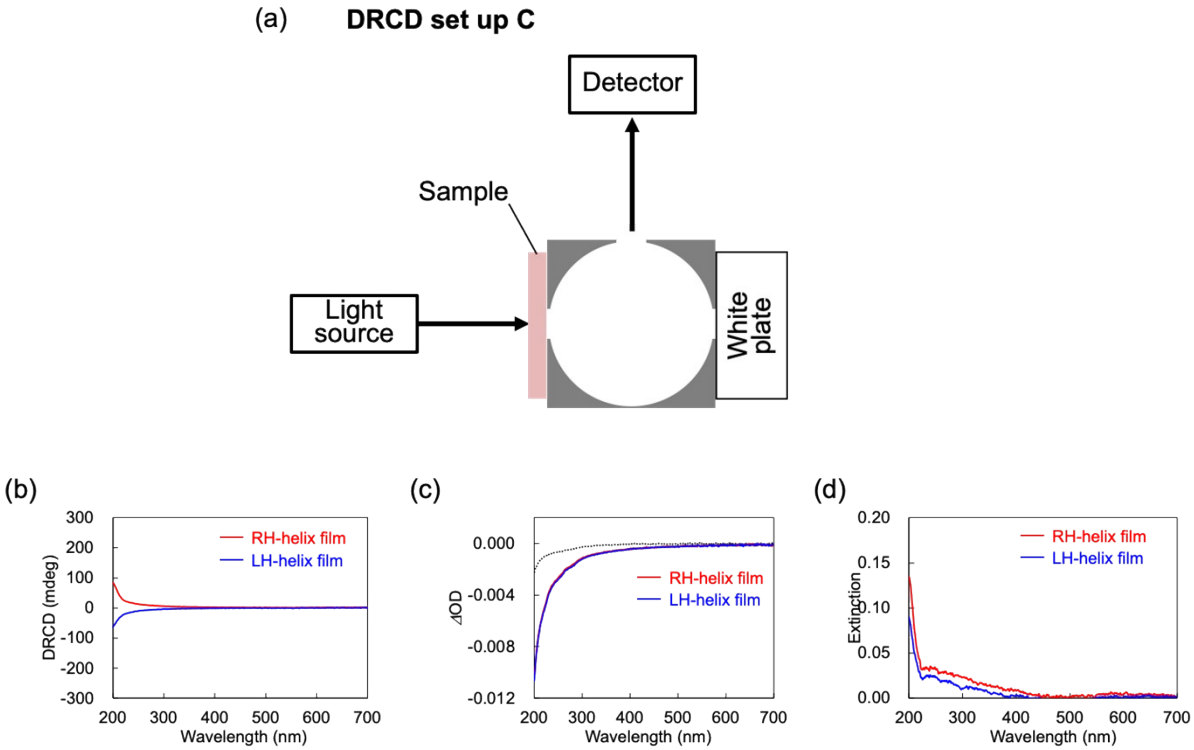

Figure S14 (a) Schematic illustration of DRCD measurement set up C. (b) CD, (c) LD, and (d) extinction spectra of silica nanohelices films.

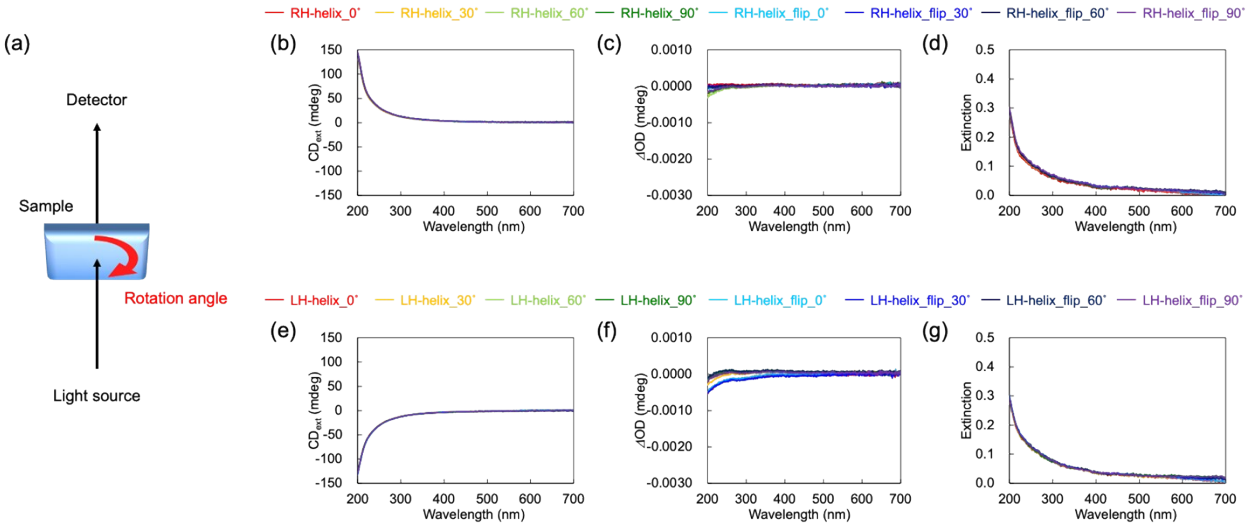

Figure S15 (a) Schematic illustration of TCD measurements at different rotational angle of the silica nanohelices films. (b,e) CD, (c,f) LD, and (d,g) extinction spectra of (b-d) RH- and (e-g) LH- helix films at different rotation angles from front side and from back (flipped) side.

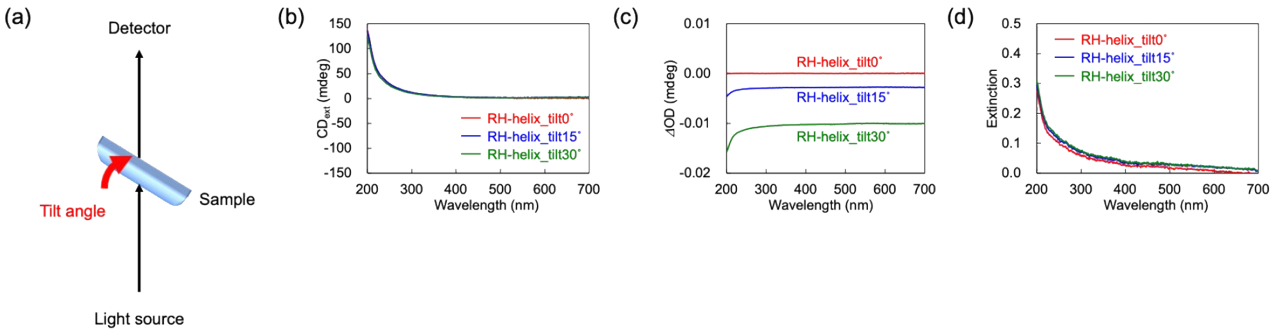

Figure S16 (a) Schematic illustration of TCD measurements at different tilt angle of the silica nanohelices films. (b) CD, (c) LD, and (d) extinction spectra of RH- helix films at different rotation angles.

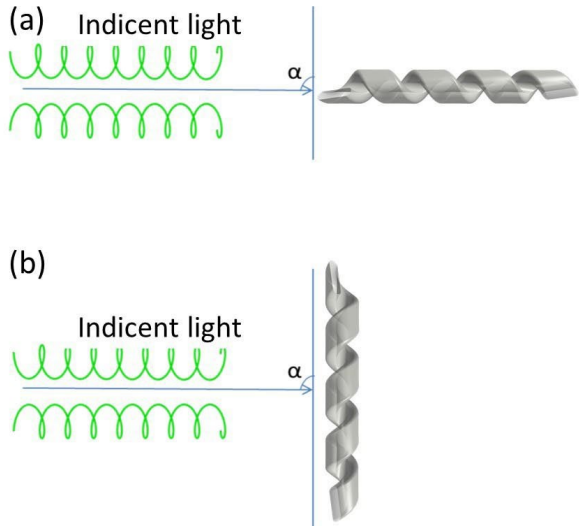

Figure S17 : Simulation on a silica helice with two orientations, (a) helix is parallel to the incident light, (b) helix is perpendiculat to the incident light.

1. A. Brizard, C. Aimé, T. Labrot, I. Huc, D. Berthier, F. Artzner, B. Desbat and R. Oda, *Journal of the American Chemical Society*, 2007, **129**, 3754-3762.
2. N. Ryu, Y. Okazaki, K. Hirai, M. Takafuji, S. Nagaoka, E. Pouget, H. Ihara and R. Oda, *Chemical Communications*, 2016, **52**, 5800-5803.
3. U. Hohenester and A. Trügler, *Computer Physics Communications*, 2012, **183**, 370-381.
4. E. D. Palik, *Handbook of Optical Constants of Solids*, 1985.